

## WELDABILITY STUDY OF DUAL PHASE AND TRANSFORMATION INDUCED PLASTICITY AUTOMOTIVE STEELS

A.K. Akela, H. Shashikumar, J.N. Mohapatra, R. Singh, D.S. Kumar, G. Balachandran

JSW Steel Ltd. Toranagallu, Karnataka, India

(Received 12 July 2022; Accepted 17 May 2023)

### Abstract

Resistance spot welding studies at varying current with an 8 mm electrode on steel grades DP980, DP690, TRIP980, and TRIP780, established that peak strength with sound weld could be achieved at a current range of 9 to 10 kA, where the nugget diameter was between 6.9 and 7.5 mm. The joint efficiency, measured as hardening ratio was highest in TRIP690 at 2.22 and for higher strength grade it was between 1.37 and 1.51. The softening ratio in the HAZ associated with tempering of preexisting martensite, was 0.86 to 0.9. Higher fusion strength was associated with alloying content that increased resistance that increased weld pool fusion that further enhanced the nugget diameter and hence the strength. The TRIP steel at high cooling rate showed martensite and retained austenite and the DP steel showed martensite content in higher grade and dispersed ferrite with martensite in the lower DP grade. The Tensile shear strength was lowest (16kN) for DP780, while for other grades it was between 20 and 22 kN. The strength enhancement in TRIP steel was due to higher weld diameter at higher current, where partial pull out failure mode was observed. At lower current, the interfacial pull out failure mode was observed with poor fusion and at high currents partial pull out at HAZ was observed. The Coach peel strength was highest at 3.2 kN for DP780, 2.2 kN for DP980, 2 kN for TRIP 690 and 1.7kN for TRIP 980 which followed the trend in TSS. The observed failure may be attributed to the high fusion strength in TRIP steel due to sound nugget and a microstructure of martensite with retained austenite. The lower strength with DP steels was attributed to low alloyed lath martensite in DP 980 and the lower grade DP780 was softer which was associated with ferrite dispersion in martensite. At very high currents, the fusion was good but there was a pull out at HAZ due to the softening associated with the tempering of preexisting martensite that influenced the failure at HAZ failure mode.

**Keywords:** Dual phase steel; Transformation induced plasticity steel; Resistance Spot welding; Microstructure; Tensile shear strength

### 1. Introduction

Advanced high strength steels (AHSS) such as Dual phase (DP) steels with ferritic martensitic microstructure and Transformation Induced Plasticity (TRIP) steels with ferrite, bainite, and retained austenite microstructure, are low carbon weldable steels that enable light weighting fuel efficient vehicles. In every vehicle about 2000 to 6000 spot welds Resistance spot welds (RSW) are made. The RSW microstructure and mechanical behavior depend on the steel composition and welding process variables that include clamping, electrode configuration, welding current, electrode pressure, time of current application, and cooling time.

AHSS has alloying element greater than 3%, which impacts the physical properties mainly resistivity and conductivity of the steel [1, 2]. Higher electrical resistivity generates higher heat and high weld pool volume in fusion zone and lower heat conductivity retains the heat for longer time [1]. The

AHSS weld fusion zone (FZ) in DP600 and TRIP780, generates high heat in weld pool that could lead to expulsion [3, 4], lack of material to fill nugget or due to solidification shrinkage, voids and weld defects and the indentation pressure is critical [1]. The weld microstructure has grain boundary allotriomorphic ferrite with Widmanstatten ferrite formation, along with martensite and retained austenite in FZ [1, 2, 4]. Increasing silicon content, increases resistivity and during cooling retards carbides promoting retained austenite [4]. Higher current influences the nugget formation and martensite transformation [5].

The FZ weld strength is influenced by the weld current and excess current result in metal expulsion [6, 7]. A decrease in electrode force increases the resistance and a higher force decreases heat and impeded nugget growth [8]. Increasing the heat input by welding current or time, reduces electrode force and the cooling rate decreases. The FZ hardness depends on the hardenability of the steels and the sheet thickness as well [9]. The HAZ of AHSS goes

Corresponding author: arbindkumar.akela@jsw.in

<https://doi.org/10.2298/JMMB220712014A>



through a softening zone due to tempering of pre-existing martensite [1, 10]. The degree of softening due to tempered martensite is a function of the martensite volume fraction, base metal chemistry, sheet thickness, heat input and welding process. Improved weld joint strength in a shorter time pulse welding causes softening associated with tempered martensite where the HAZ is minimized [10]. The amount of retained austenite in the weld metal reduces after welding in TRIP steel compared to the base metal [11]. TRIP steel with retained austenite, increases amount of austenite in weld metal compared with the base metal. Regions in the HAZ, where the peak temperatures during welding reaches the inter-critical ( $\alpha + \gamma$ ) temperature region contains higher amounts of retained austenite after welding compared to other regions in the heat affected zones [12]. The subcritical heat affected zone has tempered martensite formation. Grade DP980 with higher content of martensite is reported to give higher softening than the lower strength grade of DP steel [13]. The mechanical behavior of the weld is characterized by tensile-shear test (TS), and coach peel (CP) test and the material in FZ fail by interfacial failure (IF) or material in HAZ by pull out failure (PF) mode [1]. In a tensile shear test, the driving force for the IF failure mode depends on the area of the weld nugget in the sheet/sheet plane [10]. Thicker sheets of DP600 fail by IF mode [14]. Higher FZ size and higher hardness decreases the tendency for the IF failure mode. Full-button pull-out fracture occurs when the weld nugget size is large, and interfacial fracture occurs, when the nuggets are small [15]. In PF failure mode, tensile stresses around the nugget cause plastic deformation across the thickness that causes some rotation [1, 10, 14, 15, 16]. The PF mode is driven by the tensile stress induced by the bending moment due to the overlapping of the two sheets and rotation of the weld nugget. The necking initiation of PF mode is decided by the hardness in the FZ and in HAZ or BM. Interfacial failure to Pullout failure mode transition is correlated to the increasing FZ size and improved toughness of the weldment by martensite tempering both in the FZ and the SCHAZ in a DP 590 steel [14]. Tensile shear test failure is decided by the shear plastic deformation of the FZ [10]. The tendency for PF failure is proportional to the ratio of the hardness of the FZ to the hardness of the pullout failure location. The DP600 and DP 780 fail at BM and DP980 fails at HAZ due to low BM hardness. AHSS with common semi-brittle fracture in hard bainitic/martensitic microstructures, can be found in the HAZ and weld nugget of relatively high alloyed DP or TRIP steels. Fracture surface in soft FZ and for IF mode exhibits near equiaxed dimples, indicating that a ductile fracture occurs under tensile stress. Higher the HAZ strength, the lower the tendency is to

fail in the PF mode.

Literature on spot welding of AHSS as mentioned above, deals with specific AHSS grades and is focused on lower strength grades and the welding process. In the present study the spot welding characteristics of a DP-980 and TRIP-980 is compared with lower strength grades DP-690 and TRIP-780. There is limited information available on the higher strength grades. The higher strength grades in the present study, in addition, has higher alloying elements than those in literature. The relation between composition and base microstructure and its correlation to weld quality has been brought out.

## 2. Experimental

Four cold rolled AHSS steel grades of 1.2 mm thickness, made at JSW Steel Ltd. were chosen for the study, namely DP-780, DP-980, TRIP-690 and TRIP-980. The chemical analysis of the base metal used for welding studies was determined using ARL 3800 spectrometer. The base metal phase constitution was established using XRD technique using PANalytical model. The RSW studies were made using type IS-800A Amada Miyachi spot weld machine, with power of 170 kVA/650V and weld checker type MM-370C (Amada Miyachi). Electrodes of 8.0 mm face diameter flat tip and a cooling water flow rate of 25 L/min was maintained. The welding machine was equipped with a medium-frequency inverter to produce dc current and operate at 50Hz frequency. RSW was carried out as per parameters shown in Table 1. The welding was carried out on identical strips overlapped as per geometrical shape of tensile shear and coach peel shown in Fig.1.

**Table 1.** Welding parameter chosen as per details shown

S No	Parameters	Values
1	Material	DP 690, DP780, TRIP 780, TRIP 980
2	Sheet thickness, mm	1.2
3	Type	3
4	Dressed face dia, mm	8
5	Force, kN	3.6 to 4.0
6	Cooling, l/min	4
7	Weld time Cy	16
8	Short hold time, cy	5
9	Long hold time cy	90
10	Welding rate (w/min)	20

The samples were welded with flat electrode face diameter of 8 mm, force varied between 3.6 to 4 kN,



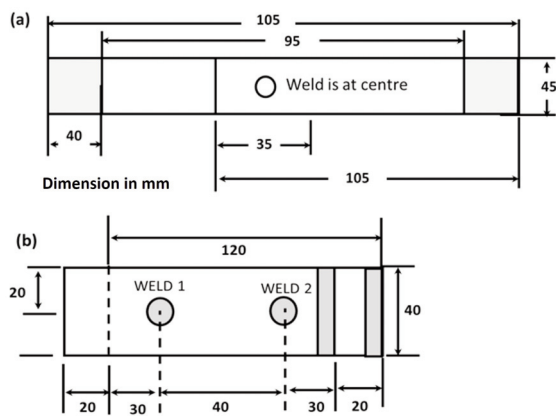


Figure 1. Schematic of (a) tensile-shear testing specimen, (b) Coach peel test specimen

a squeeze time of 60 cycle, welding time of 16 s and hold time of 90 s. The welding current varied between 5 to 13 kA. At each current value, three separate specimens in each steel, were welded. While two samples were used for tensile test, the third sample was used for weld metallography and hardness evaluation.

The samples were drawn along the direction of rolling. The current ranges were identified by determining the lowest welding current that produced the minimum acceptable weld size. Then, the current was gradually increased till the weld metal expulsion. The range of current between  $I_{\min}$  and  $I_{\max}$  was regarded as the welding current range. After the RSW, the samples were tested for nugget diameter (in mm) of weld joints with respect to weld current. Welded specimens were sectioned in half and the optical weld microstructures were observed using model DSX-510, make OLYMPUS microscope along with base metal microstructure. The tensile-shear strength (TSS) test was conducted on the Zwick RKP-250 make universal testing machine at constant strain rate of 0.008/s. Vickers micro-hardness across the weldment was measured on polished sample measured across the cross-section, using a HX-40 model microhardness Tester of Zwick/Roell,

Germany, with a normal load of 0.5 kg and application of load for a dwell time of 10 second. The test welds were peeled open and the weld size was measured using caliper. The failure features of the tensile shear test and coach peel tests were recorded.

### 3. Results and Discussions

The present study examined the spot welding characteristics of 1.2 mm thick steel strips of two grades each of a cold rolled DP steels (DP-780 & DP-980) and TRIP steels (TRIP-690 & TRIP-980) produced at JSW Steel as in Table 1. The effect of steel composition, welding parameters and their influence on strength in the FZ, and HAZ that influenced the weld failure were examined.

#### 3.1. Base Material Characteristics

The carbon equivalent, CE varied between 0.46 and 0.61 as in Table 1 [13]. The high strength steels DP 980 and TRIP 980 were relatively more difficult to weld due to higher CE. Both the DP and TRIP steels had Nb content between 0.01 to 0.07%, which promoted finer grain sizes in the base metal as shown in Fig. 2. The DP-980 had 1% higher Mn content than DP-780, which enlarged austenite field that resulted in larger fraction of martensite that resulted in higher hardness in the weld FZ. The higher alloying elements in DP-980, and TRIP 980 had the C-curve shifted to right resulting in martensite at lower cooling rate. The DP-780 had 0.17% Mo, which was a solid solution strengthener that enhanced bainite. TRIP 980 had 0.05% higher studies carbon than TRIP 690 which enhanced martensite and retained austenite. The Si content in TRIP 690 was 1.2% and TRIP 980 was 1.5%, which suppressed the carbide formation that promoted retained austenite and enhanced higher heat generation during spot welding.

The higher alloying content in AHSS (Table 1) enhanced resistivity and the alloying decreased thermal conductivity which created weld pool at faster rate and reduced cooling rate that influenced microstructure [1]. Excessive or uncontrolled heat

Table 2. Composition of the steels studied

Grade	wt. %													CE
	C	Mn	Si	S	Al	P	Ti	Nb	Cr	Mo	V	Cu	Ni	
DP-780	0.1	2.02	0.37	0.002	0.071	0.011	0.053	0.07	0.02	0.168	0.005	0.005	0.005	0.48
DP980	0.085	3.12	0.2	0.003	0.078	0.018	0.017	0.046	0.022	0.002	0.004	0.006	0.01	0.61
TRIP 690	0.2	1.5	1.2	0.004	0.062	0.028	0.03	0.01	0.018	0.01	0.001	0.006	0.008	0.46
TRIP 980	0.25	2	1.5	0.004	0.45	0.03	0.03	0.04	0.023	0.01	0.001	0.011	0.009	0.59

Carbon Equivalent(CE) =  $C + Mn/6 + (Cr + Mo + V)/5 + (Cu + Ni)/15$  (as per International Institute of Welding)



generation resulted in undesirable weld metal expulsion [4]. Higher strength steels were prone for lower contact and hence higher electrode force may be required [4]. A current range higher by 1 kA may be required for AHSS compared to other structural steel [1]. Use of higher force may end in electrode indentation, which had to be controlled below 25%

**Table 3.** Volume fraction of various phases of as-received samples of DP & TRIP steels

Steel	Phases in %			
	Ferrite	Martensite	Austenite	Pearlite/Bainite
DP 780	56	28	4	12
DP980	52	37	3	8
TRIP690	67	--	9.3	23.7
TRIP980	49.9	--	17.4	32.7

$HV_{FZ} = 630 CEY + 188$ ;  $H_M = 884(1 - 0.03 C_2) + 294$

[1]. Very high indentation may sometime act as stress risers [7, 9].

There was a fine distribution of white martensite phase in a fine grained brown bainite and gray ferrite matrix (Fig.2). The DP steels had higher fraction of soft gray ferrite phase and harder phases than TRIP steel as in Table 3. The hardness and strength were influenced by the harder bainite, martensite in Table 3. The presence of higher retained austenite in the TRIP steels was evidenced in the XRD analysis in Fig. 3. The base metal mechanical properties is shown in Table 4 and their stress-strain curves are shown in Fig. 4.

### 3.2. Preferred Process Parameters for Spot Welding

The combination of current, load and time ensured stronger weld in TRIP than DP steel as shown in Table 5. The current range varied between 5 kA and 13 kA depending on the steel grade, as in Table 5. The lower

**Table 4.** Mechanical properties of the base material steels studied

Steel Grade	Measured Hardness (HV <sub>FZ</sub> )	Calculated Hardness, HV <sub>FZ</sub>	YS (MPa)	UTS(MPa)	%E	YS/UTS
DP-780	440+17	418.24	574+13	791+35	19.5+2	0.7
DP-980	472+15	446.83	714+21	1040+42	11.4+3	0.66
TRIP-690	554+21	504.62	422+17	693+17	43+4	0.62
TRIP-980	566+29	604.24	467+20	945+33	35+3	0.51

Calculated Hardness,  $HV_{FZ} = 630 CEY + 188$   
 Where [12], HV<sub>FZ</sub> is fusion zone hardness and CEY is carbon equivalence calculated  
 $CE_Y = \%C + A(C) \{ (5 \%B + \%Si/24 + \%Mn/6 + \%Cu/15 + \%Ni/20 + \% (Cr + Mo + Nb + V)/5) \}$   
 Where, parameter  $A(C) = 0.75 + 0.25 \tanh [ 20 (\%C - 0.12) ]$

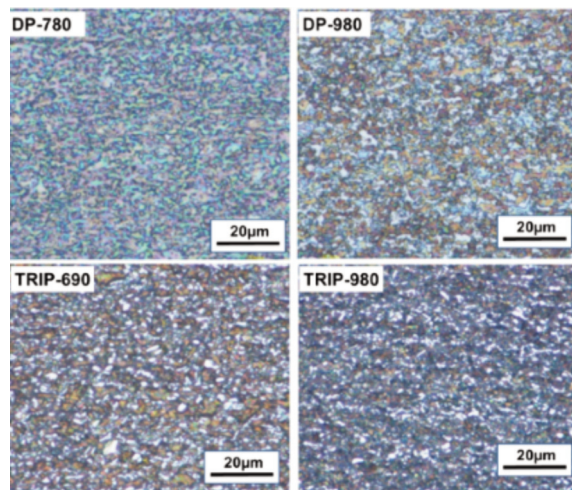


**Figure 2.** Microstructure of DP 780 and DP 980 in Nital and LePera etching respectively [Gray - ferrite; brown - bainite; white - martensite or retained austenite]

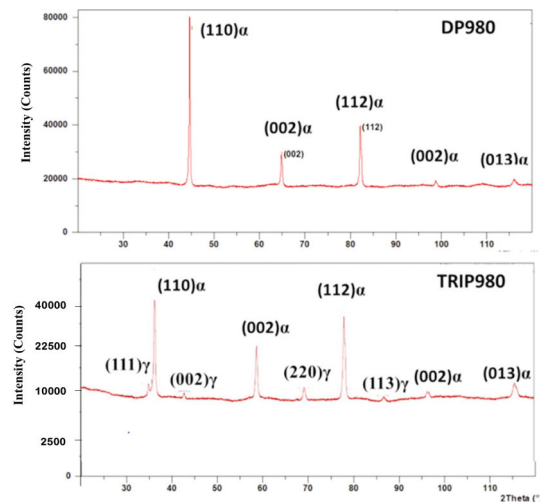


**Figure 3.** XRD analysis of typical DP and TRIP steel base metal of equivalent strength showing presence of minor austenite peaks in TRIP steel and the absence of the same in DP steel

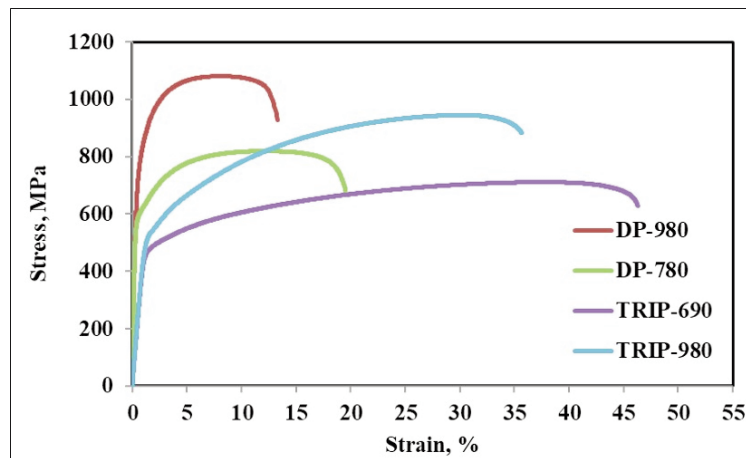


Figure 4. Engineering stress strain diagram of the base metal

limit was decided by the minimum weld size and the upper limit was decided by the expulsion. The lowest current was 5 kA for DP780 with lower alloying content and the highest current of 11 kA for both in TRIP 980 and DP 980 with higher alloying. The range of current for expulsion of metal [3, 4] during spot welding of AHSS was found to be between 9.5 and 12.5 kA for a material thickness of 1.5 mm and a welding time of 10 cycles [18] similar to that in the present study. The weld strength was highest for TRIP 980 followed by DP980 due to the higher alloying elements, which enhanced the steel resistance that promoted larger weld pool and associated nugget diameter.

The minimum weld size was 4.38 mm in thickness ( $4\sqrt{\text{thickness}}$ ) for the sheet thickness of 1.2 mm [12] and the actual welding was carried out with a 8 mm

diameter electrode. The RSW of DP and TRIP steel samples at a current of 9 kA showed that the fusion buttons were sound with smooth surface morphology in all the grades (Fig. 5). The diameter of the weld fusion zones for the different grades, was measured as shown in Fig. 5. The weld diameter was reported to be a measure of weld strength [5]. It was seen that the nugget diameter increased for TRIP steels compared to DP steel, due to its larger weld pool associated with higher resistance associated with higher alloying elements. The fusion zones in all the grades were sound and integral, without any shrinkage cavity or defect in the weld surface nugget suggesting that weld quality for the chosen parameters produced good quality welds (Fig. 6).

Weld nugget microstructures in FZ and HAZ in the conventional RSW at a 10 kA was compared for

Table 5. Welding current (kA) range and the highest strength (kN) level

Grade	Total Alloying elements %	Weld Start current (kA) $I_{\min}$	Transition of interfacial to button pull-out failure (kA)	Highest strength (kN)	Expulsion Start (kA) $I_{\max}$	Sticking Start (kA)
DP 780	2.8	5	10	18.3	11	12
DP 980	3.526	5	11	24	12	12
TRIP 690	2.877	5	9	22.92	10	12
TRIP 980	4.108	5	10	24.5	11	12

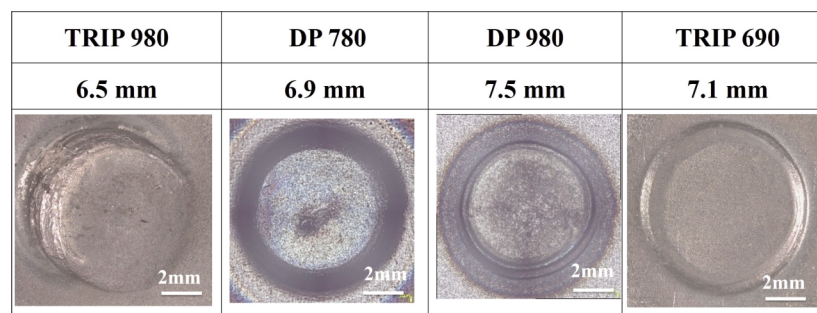
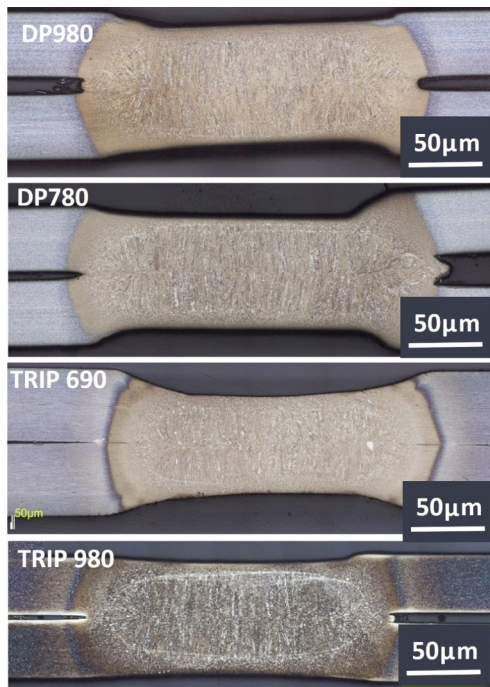


Figure 5. Surface morphology indentation of AHSS at 10 kA



**Figure 6.** Resistance spot welding of steels studied at 10kA showing the joint region can be divided into three distinct microstructural zones including BM, HAZ and FZ

all the grades as in Fig. 6. The microstructure showed a fine equiaxed grain structure close to the surface, followed by columnar grains grown from the surface towards the core with a crystal meeting zone. The core region was completely free of any defects such as shrinkage porosity, weld discontinuities, cracks etc. The fineness of the columnar grains was an indicative of the solidification of liquid pool at a high cooling rate. The electrode force was adequate as minor bulging of squeezed metal was seen between the sheets welded. In the DP780 steel, a small discontinuity was observed at the edges.

The steels were weldable over a wide range of welding current and it was seen that the nugget

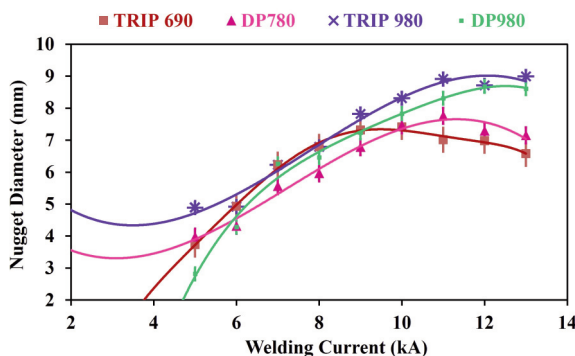
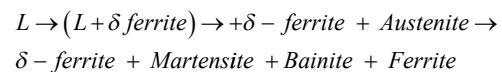


**Figure 7.** Effect of welding current on nugget diameter with acceptable current range

diameter increased from 6 kA and 11 kA as in Fig. 7, which ultimately improved the weld strength. The nugget diameter peaked at an optimum current of 11kA. Above the optimum current the decrease in nugget diameter was attributed to the expulsion [1, 6, 7, 9, 12, 13]. Expulsion occurred when the molten metal from the molten weld pool experiences a force caused by weld nugget expansion (growth) exceeding the applied electrode force [6, 8, 12]. The weldment diameter was larger than the minimum required by standard [ $4\sqrt{\text{thickness}}$  or  $5\sqrt{\text{thickness}}$ ] [12, 13].

### (c) Resistance Spot Welding Characteristics:

The macrostructure of the steel (Fig. 8(a)) and hardness across FZ and HAZ of the steel BM, FZ and HAZ microstructures are revealed in Fig. 8(b)-(c). The micro-hardness measurements, taken across the weld cross section in samples welded at 10 kA current, is shown in Fig. 8(b-c). The weld FZ hardness was twice that of the base metal hardness as in Fig. 8(b)-(c). The TRIP 980 and TRIP 690 showed the highest hardness due to the higher amount of martensite and retained austenite formed, in these grades. The higher alloying element, TRIP effect added to the base martensite hardness in FZ. The hardness of DP780 showed lower hardness than DP980 and the TRIP 690 showed higher hardness than DP980 due to lower alloying content. The weldment macrostructures for both DP and TRIP steels showed fine equiaxed grains nucleated at the copper surface followed by columnar grains growing from the sheet surface. This was due to the solidification of the weld pool due to heat transfer on the metal surface opposite to metal surface as in Fig. 8(a). The fusion zone showed cast structure and the HAZ showed the heat-treated microstructure. The microstructure was governed by solidification phase transformation where it followed from liquid weld pool (L) to other phases:



The critical cooling rate for martensite formation,  $v$  (K/h), for the steels was given by [12],

$$\log(v) = 7.42 - 3.13 C - 0.71 Mn - 0.37 Ni - 0.34 Cr - 0.45 Mo$$

It was found that when a critical cooling rate was more than about 5 K/h, there would be the formation of martensite in the fusion zone. The fusion zone showed lath martensite microstructure and the fusion zone hardness ( $HV_{FZ}$ ) was given by:

$$HV_{FZ} = 630 CE_y + 188$$



Where, the carbon equivalent,  $CE_y$  as a function of steel composition.

$$CE_y = \% C + A \left( \begin{array}{l} \% Si / 24 + \% Mn / 6 + \\ \% Cu / 15 + \% Ni / 20 + \\ (\% Cr + \% Mo + \% Nb + \% V) / 5 \end{array} \right) \quad (1)$$

Where, the parameter,

$$A(C) = 0.75 + 0.25 \tanh [20 \% C (\% C - 0.12)] \quad (2)$$

The FZ of TRIP 690 and TRIP 980 showed martensite and retained austenite phases. Higher amount of retained austenite with martensite increased the hardness of the fusion zone. The TRIP effect ensured higher hardness than DP steel. The martensite hardness was also a function of carbon content and alloying elements. The microsegregation associated with cellular solidification enhanced the retained austenite streaks embedded with martensite laths. The fusion zone consisted of large lath type martensite grains [Fig. 9 & 10]. In TRIP steel, the microstructure showed bainite and martensite due to

the presence of high Si content. The white streaks along the laths were retained austenite which showed TRIP effect [Fig.9].

At the HAZ, the TRIP980 steel showed lath type martensite and TRIP690 had bulky martensite in the HAZ. It exhibited lower fraction of retained austenite near the base metal due to transformation to martensite. The percentages of ferrite, retained austenite and martensite changed along the HAZ thickness. The measured hardness in one half sections of the weld zone, is shown in Fig. 8(c). The weld strength was influenced by the hardenability and solid solution strengthening by the Mn and Si contents. The HAZ in a AHSS weldment may be divided into three. The upper critical HAZ, where temperature was above  $A_{c3}$ , where coarse grained structure with martensite formation in TRIP780 [12]. Intercritical HAZ, where the temperature was between  $A_{c1}$  and  $A_{c3}$ , where ferrite and austenite were formed, which on fast cooling transformed the HAZ to martensite, bainite, pearlite or bainite. Sub-critical HAZ below  $A_1$ , where the martensite or bainite formed initially got tempered resulting in a lower hardness than BM in a narrow

**Table 6.** Hardness characteristics of resistance spot welds in 1.2 mm thick steel sheets [12]

Grade	Referred [12] (1.5 mm)	HV <sub>BM</sub>	HV <sub>HAZ</sub>	HV <sub>FZ</sub>	Hardening Ratio (HV <sub>FZ</sub> /HV <sub>BM</sub> )	Softening ratio (HV <sub>HAZmin</sub> /HV <sub>BM</sub> )
DP780	1.68	298	257	440	1.47	0.86
DP980	1.9	343	312	472	1.37	0.9
TRIP 690		251	218	554	2.22	0.86
TRIP 980		373	329	566	1.51	0.88

Weld efficiency: Hardening Ratio = (Hardness)<sub>FZ</sub> / (Hardness)<sub>Base Metal</sub>;  
Softening Ratio = (Hardness)<sub>min</sub> / (Hardness)<sub>Base Metal</sub>

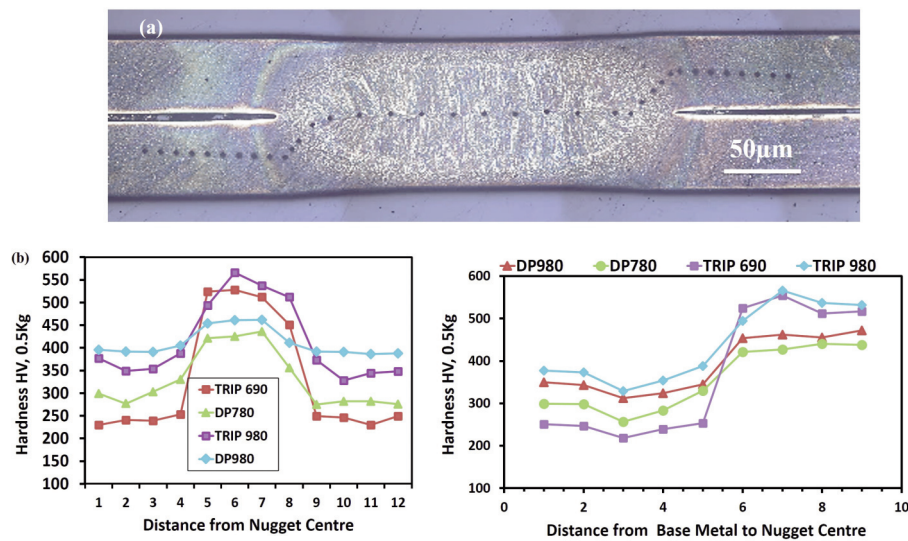


**Figure 8.** The location of micro-hardness indentations (a) and micro-hardness profiles in the entire cross-section of spot weld (b) and hardness on one half of weld nugget (c)



zone [12]. The martensite content in a HAZ increased with increase in heating temperature. It was seen that there was a weld softness observed in the HAZ towards the base metal zone (Fig.8(c)) similar to other studies [16]. The softness was associated with the tempering of the preexisting martensite in the steel as shown in Fig. 8(c) [12]. This softness in HAZ led to pull out failures. The lowering of hardness in the HAZ was related to grain growth, and the softening in a narrow range in the subcritical heat affected zone was due to the tempering of the pre-existing martensite in the steel. Depending on the chemical composition of AHSS and the initial BM microstructure, the hardness profile of spot welds of carbon steels may exhibit hardening in FZ and softening in the HAZ. The hardening ratio and softening ratio, an equivalent of weld efficiency is given in Table 6 [12]. The hardening ratio for TRIP steel was higher than DP steel, which may be attributed to higher relative hardness between the FZ hardness and the base metal.

The TRIP 980 steel showed comparable hardening ratio marginally higher than DP steel due to higher hardness of base metal with highest alloying with Mn and Si. The hardening ratio for TRIP690 was higher due to the lowest base metal hardness. In fact, because of this grade's strong intrinsic hardenability, undesirable hard microstructures could be produced quite quickly in the heat affected zone (HAZ) of welded joints [19].

The predicted hardness and the measured hardness of the welds are shown in Table 4. In the DP steels, the measured hardness was higher than calculated hardness probably due to finer grain size, as the equation did not have a grain size factor. In addition, the equation did not factor in the effects of retained austenite. In the DP steel, the martensite fraction decided the hardness. In the case of TRIP steels, the measured hardness was either equivalent or lower than theoretical hardness. This may probably be due to the presence of retained austenite phase. The DP

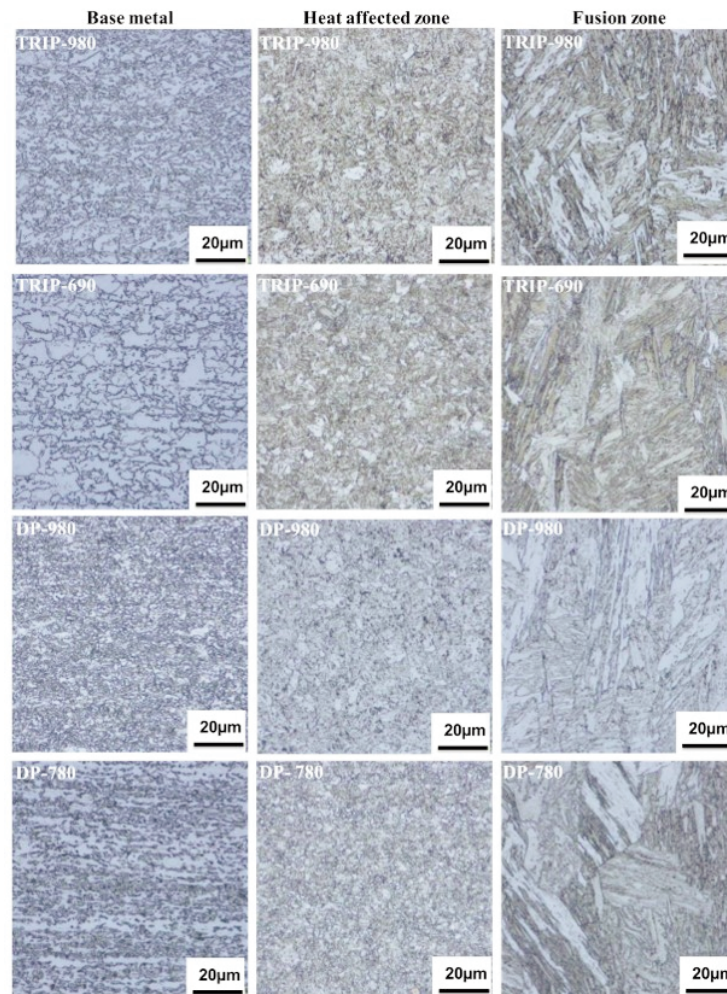


**Figure 9.** The optical micrograph of weld sample including base metal, heat affected zone and fusion zone.spot weld (b) and hardness on one half of weld nugget (c)

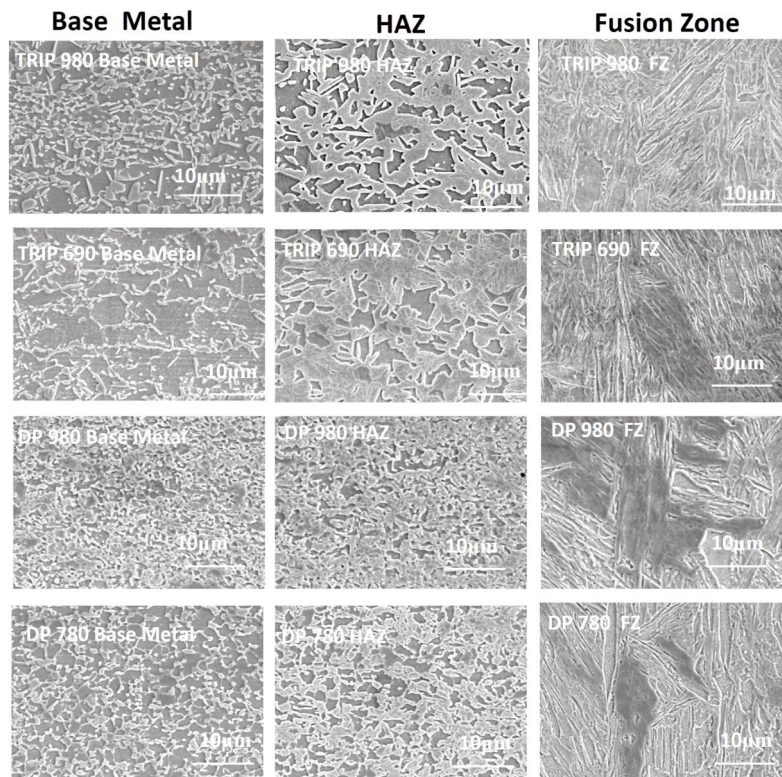


Figure 10. The SEM micrograph of the weld sample including base metal, heat affected zone and fusion zone

steel base metal had martensite dispersion in ferrite. It was reported in thin samples 0.8 to 2 mm thick AHSS, the cooling rate at the FZ was of the order of 8000 to 2000 °C/s [5]. The critical cooling rate for AHSS was of the order of 500 °C/s. Hence, the formation of martensite was predominant in TRIP 980 and TRIP 690 which made them brittle. The DP980 and DP780 grades had lower hardness associated with lower alloying content.

The HAZ went to temperature below  $A_{c1}$  temperature, and the cooling rate was still fast enough

to form martensite. The microstructure showed island of ferrite [Fig. 9 than HAZ] which was the reason the steel was softer compared to FZ. The extent of martensite decided the hardness (Fig. 8(b)). Peak temperatures at HAZ during welding was typically below the martensite tempering temperature (i.e., < 200 °C) earlier reported by Hsu et al. [11]. Within the HAZ, the peak temperature was well above  $A_{c3}$ , resulting in complete austenitization and grain growth.

Spot welds in automotive structures in service,

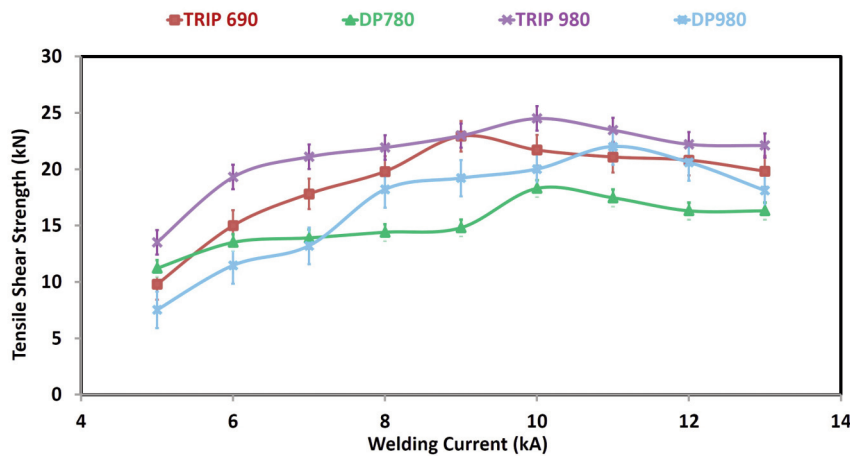


Figure 11. Tensile shear strength increases with increase in current and above a peak current the shear strength decreases due to weld expulsion

experienced significant shear loading, due to the relative displacement hence the Tensile shear strength (TSS) was measured. The TSS of the weld measured the force experienced by the joint for failure. Larger the TSS, better was the strength. The TSS increased with increasing current, peaking at about 10 kA current, as in Fig.11, due to the better bonding in the weld. At very high currents the TSS taper due to expulsion [17]. The TSS was found to increase in proportion to nugget diameter [5]. The highest weld strength was observed in TRIP980 and TRIP 690 and

the least with DP780 probably due to higher retained austenite in the steel. The TSS test failure mode at lower current of 5 kA showed interfacial pull out of the weld fusion zone (Fig. 12), associated with lower strength at the fusion zone. At higher weld current of 9 kA, where the strength was highest the failure transformed to partial pull out fracture mode. At still higher current of 9 kA, the failure mode transformed to partial pull out especially initiated in the HAZ. The softer tempered martensite initiated the failure due to its soft strength. AHSS predominantly fail by

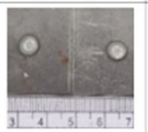
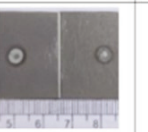
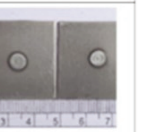
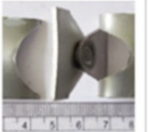
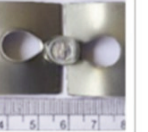
Weld Current	Failure mode were observed after the Tensile-Shear Test			
	TRIP 980	TRIP 690	DP 780	DP 980
5 kA (Interfacial)				
9 kA (Partial Pullout fracture)				
	Failure mode were observed after coach peel test			
	TRIP 980	TRIP 690	DP 780	DP 980
5 kA (Interfacial)				
9 kA (Partial Pullout fracture)				

Figure 12. Failure Modes in the tensile shear test samples and coach peel test at 10 kA

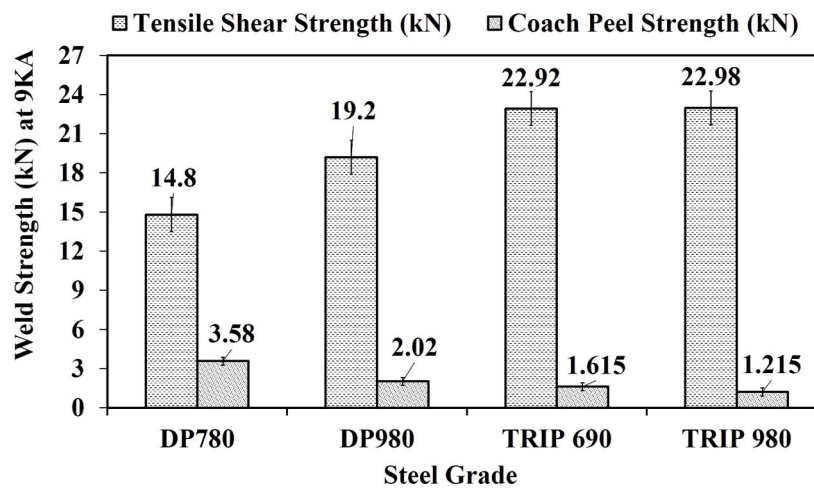


Figure 13. Tensile shear & Coach peel strength at 10 kA current

interfacial failure mode [10]. In TRIP steels there was the formation of retained austenite along the martensite laths that enhanced the TSS. In DP980, as well as more martensite in FZ enhanced strength, while in DP780 the presence of ferrite deteriorated the strength.

The coach peel test on the steel, showed highest strength in TRIP980 and TRIP690. The lowest strength was realized with DP780 steel. This followed the trend same as that of the TSS (Fig. 12). The peel test at 5 kA showed interfacial failure in peel test, which implied poor weld strength. In DP800 and TRIP800 welds, the failure mode had a very strong influence on both peak load and energy, failure energy was significantly affected by the way in which spot weld fails [10, 15]. The tortuosity of crack path in the pullout mode would dissipate more energy and was preferable to the interfacial failure mode, which did little to deflect the direction of crack propagation. Spot welds with good mechanical performance had spot welds that failed in the pullout mode, rather than in the interfacial mode [10, 15].

The TRIP980 and TRIP 690 had the highest strength TSS and lowest coach peel resistance at 10 kA (Fig.13) welding current in accordance with the weld hardness of FZ shown in Fig. 8(b), where the microstructure in Fig. 9 showed, lath martensite with retained austenite. The DP steel grades at same conditions showed lower shear strength and higher coach peel strength (Fig.13) due to lower hardness of FZ as in Fig.8(b) with softer bainitic fraction with martensite fraction Fig. 9.

#### 4. Conclusions

1. Resistance spot welding characteristics of the steel grades DP780, DP980, TRIP690, and TRIP980 steel grades, with an 8 mm electrode, over a range of current, showed that the weld strength peaked for a current range of 9 to 10 kA current, where nugget diameter was high and harder martensite and retained austenite phases are formed.
2. The weld strength was highest in TRIP steel associated with higher alloying content that increased the steel resistivity that resulted in the ease of molten pool formation in Fusion zone. At low current inadequate fusion resulted and at very high currents there was metal expulsion.
3. The weld fusion zone at 10 kA gave sound nugget with nugget diameter varying between 6.5 and 7.5. The weld microstructure showed columnar grains indicative of high cooling rate during solidification where columnar grain was observed.
4. TRIP steel showed lath martensite with bainite with retained austenite which enhanced the hardness. The DP steel showed lath martensite with low alloying content and some ferrite was retained in

lower DP grade. The HAZ in the TRIP steel showed softening associated with tempering of pre-existing martensite.

5. Hardness measurement across the weld nugget showed that the weld efficiency as measured by hardening ratio was 2.22 for TRIP690 and for other grades it was between 1.37 and 1.51. The softening ratio associated with tempering of pre-existing martensite was found to be between 0.86 and 0.9. The measured hardness was higher than theoretically predicted hardness probably due to the absence of grain size and presence of retained austenite fraction in the steel.

6. Tensile shear strength and Coach Peel test were done in RSW done at 10 kA current. The tensile shear strength was lowest for DP780 where the strength was lowest (16kN) while it was between 20 and 22 kN for other grades. The Coach peel strength was highest for DP780 at 3.2kN, DP 980 at 2.2 kN, TRIP690 at 2kN, and TRIP980 at 2.2 kN.

7. The observed failure in the steel in the tests could be related to the weld fusion zone and HAZ. Interfacial failure was observed at lower currents due to inadequate fusion zone formation. TRIP steel with high TSS could be obtained with martensite and bainite with retained austenite. Lower TSS strength and Peel strength in DP steel was associated with low strength lath martensite. In lower DP grade, the presence of ferrite softened the weld zone. When the weld zone was strong at high currents with sound nugget, pull out failure occurred in the HAZ which was softer, associated with the tempering of pre-existing martensite.

#### Author contributions

*Writing-original draught and investigation: A.K. Akela, testing: H. Shashikumar, J.N. Mohapatra, writing-review: R. Singh, D.S. Kumar, and editing: G. Balachandran*

#### Data availability

*The research that provided the data for the findings of this study was carried out at JSW Steel Ltd.*

#### Conflict of interest

*The authors declare that they do not have any conflicts of interest.*

#### References

- [1] M. Tumuluru, Some considerations in the resistance spot welding of dual phase steels, Process International Seminar on Advances in Resistance Welding, September 24–26, Toronto, Canada. Weston, Ontario, Canada, 2008.



- [2] D. J. Radakovic, M. Tumuluru, An evaluation of the cross-tension test of resistance spot welds in high strength dual phase steels, *Welding Journal*, 91 (1) (2012) 8S–15S.
- [3] S.S. Nayak, Y. Zhou, V.H. Baltazar Hernandez, E. Biro, Resistance Spot Welding of Dual-phase Steels: Heat affected zone softening and tensile properties, Research, Proc. 9th International Conference, Trends in Welding June 4–8, Chicago, Illinois, USA, 2012, p. 641-649.
- [4] M. Amirthalingam, Microstructural Development during Welding of TRIP Steels, PhD thesis of Delft University of Technology, Netherlands, 2010, p. 65-83.
- [5] H. Oikawa, G. Murayama, T. Sakiyama, Y. Takahashi, T. Ishikawa, Resistance Spot Weldability of High Strength Steel (HSS) Sheets for Automobiles, Nippon Steel Technical Report No. 95 January 2007, UDC 621.791.763.1:669.14.018.292
- [6] H. Ghazanfari, M. Naderi, Influence of welding parameters on microstructure and mechanical performance of resistance spot welded high strength steels, *Acta Metallurgica Sinica (English Letters)*, 26 (5) (2013) 635-640.  
<https://doi.org/10.1007/s40195-013-0076-1>
- [7] N. T. Williams, J. D. Parker, Review of resistance spot welding of steel sheets Part 1 Modelling and control of weld nugget formation, *International Materials Reviews*, 49 (2) (2004) , 45-75.  
<https://doi.org/10.1179/095066004225010523>
- [8] A. Arumugam, A. A. Baharuddin, Effect of force control during spot welding on weld properties, *International Journal of Scientific and Research Publications*, 4 (8) (2014) 1-6. ISSN 2250-3153.
- [9] M. Tumuluru, Resistance spot welding of coated high strength dual-phase steels, *Welding Journal*, 85 (8) (2006) 31-37.
- [10] T. Koichi, O. Yasuaki, I. Rinsei, Development of next generation resistance spot welding technologies improving the weld properties of advanced high strength steel sheets, JFE Technical Report No. 20 (Mar. 2015), Originally published in JFE GIHO No. 34 (Aug. 2014), p. 8–13.
- [11] T. I. Hsu, L. T. Wu, M. H. Tsai, Resistance and Friction Stir spot welding of a dual phase (DP-780) – a comparative study, *The International Journal of Advanced Manufacturing Technology*, 97 (2018) 2293-2299.  
<https://doi.org/10.1007/s00170-018-2056-0>
- [12] M. Pouranvari, S. P. H. Marashi, Critical review of automotive steels spot welding process, structure and properties, *Science and Technology of Welding and Joining*, 18 (5) (2013) 361-403.  
<https://doi.org/10.1179/1362171813Y.0000000120>
- [13] M. Ibraheem Khan, Spot Welding of Advanced High Strength Steels, A thesis, Master of Applied Science in Mechanical Engineering, Waterloo, Ontario, Canada, 2007, p. 1-115.
- [14] I. Ali Soomro, S. Rao Pedapati, M. Awang, Double pulse resistance spot welding of dual phase steel: parametric study on microstructure, failure mode and low dynamic tensile shear properties, *Materials*, 14 (802) (2021) 1-19.  
[https://doi.org/10.3390/ma14040802\\_](https://doi.org/10.3390/ma14040802_)
- [15] C. Ma, D.L. Chen, S.D. Bhole, G. Boudreau, A. Lee, E. Biro, Microstructure and fracture characteristics of spot-welded DP600 steel, *Material Science and Engineering A*, 485 (2008) 334-346.  
<https://doi.org/10.1016/j.msea.2007.08.010>
- [16] N. Zhong, X. Liao, M. Wang, Y. Wu, Y. Rong, Improvement of microstructures and mechanical properties of resistance spot welded DP600 steel by double pulse technology, *The Japan Institute of Metals, Materials Transactions*, 52 (12) (2011) 2143-2150.  
<http://dx.doi.org/10.2320/matertrans.M2011135>
- [17] P. R. Spena, M. De Maddis, G. D'Antonio, F. Lombardi, Weldability and monitoring of resistance spot welding of Q&P and TRIP steels, *Metals* 6 (11) (2016) 1-15. <http://dx.doi.org/10.3390/met6110270>
- [18] M. Pouranvari, Metallurgical challenges in resistance spot welding of advanced high strength steels, 3rd Iron and Steel Symposium (UDCS'17) Karabuk-Turkey 3-5 April 2017 (2017) 667.
- [19] S. Oktay, P.E. Di Nunzio, M.C. Cesile, K. Davut, M.K. Şeşen, Effect of coiling temperature on the structure and properties of thermo-mechanically rolled s700mc steel, *Journal of Mining and Metallurgy, Section B: Metallurgy*, 58 (3) (2022) 475 – 489.  
<https://doi.org/10.2298/JMMB2203040280>



## STUDIJA ZAVARLJIVOSTI DVOFAZNOG ČELIKA I ČELIKA SA TRANSFORMACIJSKI INDUKOVANOM PLASTIČNOŠĆU U AUTOMOBILSKOJ INDUSTRIJI

A.K. Akela, H. Shashikumar, J.N. Mohapatra, R. Singh, D.S. Kumar, G. Balachandran

JSW Steel Ltd. Torangal, Karnataka, Indija

### Apstrakt

Studije elektrootpornog tačkastog zavarivanja pri promenljivoj električnoj struji i sa elektrodom od 8 mm na čelicima DP980, DP690, TRIP980 i TRIP780, pokazale su da se maksimalna čvrstoća na dobro zavarenom spoju može postići kada je struja u opsegu od 9 do 10 kA i kada je prečnik zavarenog otiska između 6,9 i 7,5 mm. Efikasnost spoja koja se merila kao odnos stvrdnjavanja, bila je najveća kod TRIP690 sa vrednošću od 2,22, dok je kod čelika sa većom čvrstoćom iznosila između 1,37 i 1,51. Odnos omekšavanja u toplotnoj zoni iznosio je između 0,86 i 0,90, a povezan je sa temperovanjem postojećeg martenzita. Veća čvrstoća fuzije povezana je sa sadržajem legura koji povećava otpor i stvara veći otisak fuzije zavarenog spoja, što dalje povećava čvrstoću. Čelik TRIP pri brzom hlađenju pokazuje prisustvo martenzita i zaostalog austenita, dok čelik DP u višem rangu pokazuje veći sadržaj martenzita, a u nižem rangu raspršeni ferit u martenzitu. Smicajna čvrstoća bila je najniža (16 kN) kod DP780, dok je kod ostalih čelika iznosila između 20 i 22 kN. Poboljšanje čvrstoće kod TRIP čelika se javlja kao rezultat većeg prečnika zavarenog otiska pri većoj struji, kada se javlja i delimično otkazivanje. Pri nižoj struji primećuje se otkazivanje interfejsa sa lošom fuzijom, a pri visokim strujama delimično izvlačenje u toplotnoj zoni utvrđeno je kao način otkazivanja. Čvrstoća ljuštenja (Coach peel strength) bila je najveća kod DP780 (3,2 kN), zatim kod DP980 (2,2 kN), TRIP690 (2 kN) i TRIP980 (1,7 kN), što prati trend rastezne čvrstoće (TSS). Primećeno otkazivanje može se pripisati visokoj čvrstoći fuzije kod TRIP čelika usled prisustva dobrog otiska i mikrostrukture martenzita sa zadržanim austenitom. Niža čvrstoća kod DP čelika pripisuje se nisko legiranom prizmenom martenzitu kod DP980, dok je niži rang DP780 bio mekši, što je bilo povezano sa disperzijom ferita u martenzitu. Pri veoma visokim strujama, fuzija je bila dobra, ali se javljalo izvlačenje u toplotnoj zoni usled omekšavanja povezanog sa kaljenjem prethodno postojećeg martenzita, što je uticalo na otkazivanje u toplotnoj zoni.

**Ključne reči:** Dvofazni čelik; Čelik sa transformacijski indukovanom plastičnošću; Elektrootporno tačkasto zavarivanje; Mikrostruktura; Smicajna čvrstoća

